EUROPHYSICS LETTERS 1 August 1997

Europhys. Lett., **39** (3), pp. 287-292 (1997)

Intermittent diffusion on the reconstructed Si(111) surface

K. Cho(*) and E. Kaxiras

Department of Physics and Division of Engineering and Applied Sciences
Harvard University, Cambridge, MA 02138, USA

(received 10 February 1997; accepted in final form 22 June 1997)

PACS. 68.35Fx – Diffusion; interface formation.
PACS. 66.30Dn – Theory of diffusion and ionic conduction in solids.
PACS. 81.15Hi – Molecular, atomic, ion, and chemical beam epitaxy.

Abstract. – The diffusion of an extra-adatom on reconstructed Si(111) surfaces is investigated using density-functional total-energy pseudopotential calculations. The diffusion path is characterized by a *basin of attraction* in which the extra-adatom is localized until an intermittent jump to a nearby basin of attraction occurs. The energy barrier between the neighboring basins is 1.12 eV, while the energy barrier within a basin is 0.56 eV. Our theoretical predictions for stable and activated configurations provide a natural explanation for the scanning tunneling microscopy images of an extra silicon atom on the Si(111)-(7 × 7) surface, which is radically different from the simple models proposed in the literature.

Atomic diffusion is the key process that controls the nature of diverse near-equilibrium and non-equilibrium phenomena, including, for instance, growth on surfaces, the formation of dendrites and voids, the motion of interfaces in microstructure evolution, and electromigration processes. The desire to understand the fundamental aspects of growth from a microscopic perspective has placed surface diffusion at center stage of recent theoretical and experimental investigations [1]. In the most direct experimental measurements of adatom diffusion on surfaces, scanning tunneling microscopy (STM) and field ion emission techniques have been able to image diffusing adatoms at successive stable or metastable positions, thus revealing a wealth of information on the microscopic atomic motion. Despite this progress, it is impossible to capture a diffusing adatom at the saddle-point configuration, and therefore the exact diffusion path is typically assumed to be a simple interpolation between initial and final configurations. Theoretical calculations of the activation energy and entropy have confirmed that in many cases these simple assumptions are reasonable and consistent with experimental measurements [1], [2]. It is also typically assumed that the adatoms vibrate with thermal amplitude near their stable and metastable configurations, until they acquire enough energy through random fluctuations to climb to the saddle-point configuration, which leads to a diffusion event.

(*) Address from September 1997: Mechanics and Computation Division, Mechanical Engineering Department, Stanford University, Stanford, CA 94305-4040, USA.

In this letter we demonstrate that extra-adatom [3] diffusion on one of the most intensively studied semiconductor surfaces, the Si(111)-(7×7) reconstruction, is rather different than might be expected from simple considerations. In fact, a naive interpretation of STM experiments (that is, assuming that a surface atom corresponds to each bright spot in the STM images) would give a completely wrong assignment for the stable and metastable extra-adatom positions, and an unrealistic picture of the actual atomic motion [4], [5]. Our description of extra-adatom diffusion on the Si(111)-(7 × 7) surface is based on extensive theoretical investigations using accurate quantum-mechanical calculations. In a nutshell, we find that extra-adatoms are trapped in regions of the surface which are large enough to allow for very rapid diffusion within that region, with occasional jumps between equivalent regions; we call this motion "intermittent diffusion" to distinguish it from the simple cases mentioned above. While the discussion here is limited to an extra-adatom on the reconstructed Si(111) surface, the concept of intermittent diffusion is applicable to a wide range of semiconductor surfaces and different adatoms: We have investigated the motion of metal adatoms on Si(111)-(7 × 7) and found similar intermittent-diffusion behavior. Moreover, several stable semiconductor surfaces have local geometries similar to the Si(111) reconstruction (*e.g.*, Ge(111)-c(2 × 8), and III-V(111) and $(\bar{1}\bar{1}\bar{1})$ surfaces with group-V trimers or group-III adatoms), where analogous behavior of extra-adatoms might be expected.

We begin with a short discussion of the important features of the Si(111)-(7 × 7) surface reconstruction. The unit cell of this reconstruction has two halves (one of them containing a stacking fault). Since the outermost atomic features within the two halves of the unit cell are identical, we concentrate on one half. Within this half unit cell the basic features are referred to as adatoms, rest atoms, dimers and corner holes, which are all illustrated in fig. 1 (a). In our calculations we employ a simpler (4×4) supercell with four adatoms and four rest atoms locally arranged in a (2 × 2) pattern, shown in fig. 1 (b). This is precisely the same local arrangement of features in each half of the (7 × 7) unit cell, but omits the dimers and the corner holes. This choice was made so that highly accurate and extensive calculations could be performed on the smaller (4 × 4) supercell. Consequently, our work does not address atomic diffusion across the dimer boundary of the (7 × 7) unit cell, which separates the two halves.

In terms of technical details, we use a four-layer slab configuration with the bottom layer fixed at bulk positions and saturated by hydrogen atoms. Slabs are separated by 12 Å. The electronic energy functional is obtained from the local density approximation to density functional theory, and minimized using the Car-Parrinello scheme [6] implemented on a CM-5 parallel supercomputer [7], [8]. Optimized non-local pseudopotentials [9] were used in the Kleinmann-Bylander separable form [10] with a plane-wave basis with 8 Ry cut-off energy, while the Brillouin-zone integrations were approximated by the Γ-point. To establish the accuracy of the calculations we performed extensive tests in a (2 × 2) unit cell containing one *intrinsic* adatom (no extra-adatoms) and one rest atom, and a correspondingly larger number of k-points which map to the Γ-point of the (4×4) supercell. We have calculated the energies of the stable configuration (the top fourfold coordinated, or T_4 position), the metastable configuration (the hexagonal threefold coordinated, or H_3 position) and the saddle-point configuration (the bridge twofold coordinated, or B_2 position) as a function of the plane-wave cut-off (with 8, 10, and 12 Ry cut-offs) and as a function of the density of Brillouin-zone sampling points (with (2,2,1) and (3,3,1) Monkhorst-Pack (MP) k-point schemes [11]). From the energies of the three configurations, we deduce an error bar of 0.05 eV for relative energy differences with an 8 Ry cut-off and a $(2, 2, 1)$ MP k-point scheme in the (2 × 2) unit cell, which is equivalent to the Γ-point of the (4 × 4) unit cell.

We investigated diffusion by placing the extra-adatom at various positions in the (4 × 4) unit cell and calculating the total energy of the system including full relaxation of all atoms

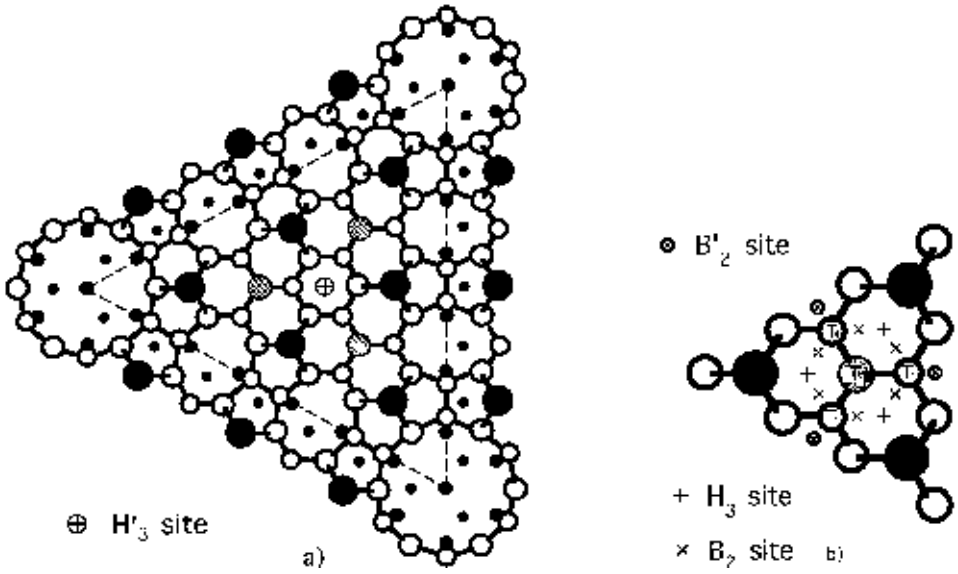

Fig. 1. – (a) Ball-and-stick model representation of the (7×7) reconstruction half unit cell. Large black circles are the adatoms, and grey circles are the rest atoms. The broken lines show the boundary of the half unit cell, and the three corner holes are at the vertices of the triangle. The symbol at the center of the figure marks the H_3'-type position which separates three neighboring rest atom sites. (b) One of the rest atom sites with three neighboring adatoms, and the high-symmetry positions of an extra-adatom, marked with different symbols.

(except those in the bottom hydrogenated layer). In fig. 1 (a) and 1 (b) we indicate with different symbols certain high-symmetry positions of the extra-adatom. The energies for these positions are given in table I. In fig. 2 we give a plot of the total-energy landscape which is an interpolation of the calculated energies at various extra-adatom positions, using an expansion in trigonometric functions with the requisite symmetries. There are some striking features in the energy landscape: Within a triangular region defined by three surface T_4 adatoms the most stable position of the extra-adatom is not on top of the rest atom dangling bond T_1, as might be expected by bond-counting arguments, or by a naive interpretation of STM images, which show a pronounced bright spot centered at the T_1 site [4], [5]. In fact, this is the position of *highest* energy within the triangular region. The most stable configuration for the extra-adatom is a B_2-type position [12], and the next lower-energy configuration is a T_4-type position. Note that, while satisfying dangling bonds is an important consideration, over-coordinated Si atoms are energetically preferred in surface geometries, as the lower energy of a T_4 *vs.* an H_3 intrinsic adatom indicates. Based on these observations, and the fact that the B_2-type, T_4-type and H_3-type positions of the extra-adatom involve higher coordination, while the T_1 position involves single coordination for the extra-adatom, it is not surprising that indeed the T_1 position is the one with highest energy.

Table I also lists the adsorption energies of an extra-adatom at various sites relative to a Si atom in vacuum. These energies are a combination of the bonding energy of the extra-adatom to the surface and the surface relaxation energy. In comparison to the energy of a single bond in the bulk (-2.32 eV), only the T_1 site has a smaller adsorption energy (-1.93 eV), while all the other sites have larger adsorption energies, including the H_3'-type site which does not have any

TABLE I. – *Energy, coordination, and bond lengths of an extra-adatom on the reconstructed* Si(111) *surface: Surface energies* ($E_{\rm sur}$) *are relative to the energy of the* (2×2) *surface and one bulk silicon atom; adsorption energies* ($E_{\rm ad}$) *are relative to the energy of the* (2×2) *surface and one silicon atom in vacuum. The* T_1 *site is on top of the grey atoms shown in fig.* 1 (a)*; the* H_3'*-type position is at the center of the triangular half unit cell as shown in fig.* 1 (a)*;* X_n*-type* ($X_n = B_2, B_2', H_3, H_3', T_4$) *positions are indicated in fig.* 1 (b).

Adatom site	$E_{\rm sur}$ (eV)	$E_{\rm ad}$ (eV)	Coordination	Bond lengths (Å)			
T_1	2.70	−1.93	1	2.29			
B_2-type	0.69	−3.94	3	2.39	2.48	2.60	
T_4-type	0.96	−3.67	4	2.46	2.47	2.55	2.55
H_3-type	1.25	−3.38	4	2.36	2.70	2.72	2.72
B_2'-type	1.81	−2.82	3	2.40	2.40	2.57	
H_3'-type	1.95	−2.68	3	2.46	2.46	2.46	

dangling bonds in its vicinity to which the extra-adatom could bind. A detailed analysis of the relaxed geometries shows that the most prominent feature of the surface relaxation when the extra-adatom is placed at various sites is the relaxation of intrinsic adatoms and in particular the weakening of their back bonds, as evidenced by their lengthening by 0.05–0.10 Å. As indicative features of the local geometry of the extra-adatom, we list in table I its coordination and bond lengths for each site. The extra-adatom has typical coordination of 3 or 4, except at the highest-energy T_1 site, and has the lowest energy when the bonds are reasonably close to the ideal Si bulk bond of 2.35 Å.

A pathway connecting the B_2-type and the T_4-type positions goes through an H_3-type position (see fig. 2), leading to an energy barrier of 0.56 eV. This is a relatively low-energy barrier, indicating fast diffusion of the extra-adatom within this region at room temperature. Consequently, the STM signature of an extra-adatom will be the result of superposing the images from the stable positions within one basin of attraction (similar to the symmetric dimer STM image on the Si(100) surface [13]). For a direct comparison to experiment, we present in fig. 3 a set of theoretical STM images (constant tip-height STM images within the Tersoff-Hamman theory [14]) of the occupied states within 2 V bias voltage, produced from the calculated electronic charge densities. Figure 3 (a) corresponds to the T_1 position, which has the highest energy, and has been suggested as the possible stable position of the extra-adatom [4], [5]. From our calculations, we find this explanation unlikely. The high energy of this position suggests that the extra-adatom visits this position extremely rarely, if ever. Instead, the extra-adatom resides in one of the stable B_2-type positions within the basin. Figure 3 (b) shows the theoretical STM image for the B_2-type stable position for the extra-adatom, which is asymmetric and rather different from the T_1 image. At room temperature, all equivalent B_2-type positions within one basin are accessible to the extra-adatom. A theoretical STM image produced by superposition of images from these equivalent B_2-type positions is shown in fig. 3 (c). In principle, a superposition of all the STM images with proper Boltzmann factors along the path must be considered, but in practice at room temperature the extra-adatom spends most of its time around the stable B_2-type positions, so that the superposition of the STM images at six equivalent B_2-type sites is an excellent good approximation. As in the case of the T_1 position (fig. 3 (a)), in this STM image the bright spot is *centered* at the geometrical center of the basin (the T_1 site), but the physical origin of this symmetric image is entirely different from the interpretation that places the extra-adatom at the T_1 site.

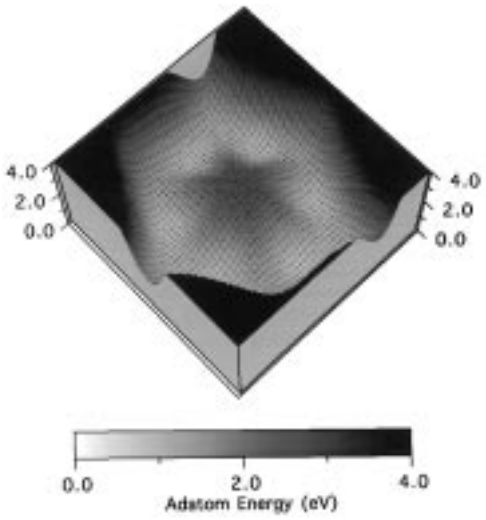

Fig. 2

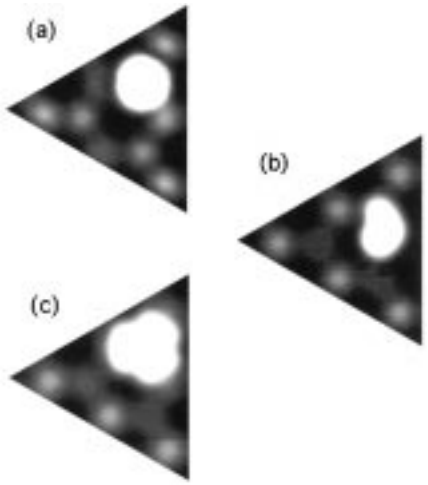

Fig. 3

Fig. 2. – The extra-adatom energy surface in the basin of attraction shown in fig. 1 (b). The energy scale is from 0.0 to 4.0 eV as indicated by the grey scale bar. At the center of the well, the T_1 site corresponds to a small mountain with sixfold rotational symmetry. Within the well there are six local minima separated by 0.56 eV energy barriers around the T_1 mountain. At the outer boundary of the well, three pathways to neighboring wells are shown with a barrier of 1.12 eV.

Fig. 3. – Theoretical STM images for different positions of the extra-adatom: (a) at the unstable T_1 position, (b) at the stable B_2-type position, (c) superposition of images from the six equivalent B_2-type positions within one basin of attraction.

We are aware of two experiments that have attempted to image extra-adatoms on the Si(111)-(7×7) surface with STM [4], [5]. In both cases, the observed image is much closer to fig. 3 (c) than to fig. 3 (a). Specifically, the experimental STM images show a bright spot *centered* at the geometric center of a triangular basin, but with distinct protrusions with threefold symmetry, as in fig. 3 (c) and in contrast to fig. 3 (a). However, it is possible that tip effects may affect the details of the experimental STM image and it is conceivable that these effects can make the image corresponding to the T_1 position appear more like our theoretical STM image from the superposition of equivalent B_2-type positions. In order to distinguish these two possibilities, we propose a low-temperature STM experiment, which should be able to image an extra-adatom in one of the equivalent B_2-type positions, whereupon the highly asymmetric image of fig. 3 (b) should be observed.

On the other hand, the extra-adatom can only move outside of a basin of attraction by overcoming a diffusion barrier of 1.12 eV, which corresponds to the B_2'-type position. This is exactly double the barrier for diffusion within one of the triangular basins of attraction, indicating that the ratio of the rate at which the extra-adatom performs diffusion events within one basin of attraction to the rate of diffusion events across basins is 10^5 at 300 °C or 2×10^3 at 600 °C (this comparison assumes that attempt frequencies and entropy factors are similar for diffusion within and across basins of attraction). Furthermore, assuming an attempt frequency of 10^{13} s^{-1}, an average time for an intermittent diffusion event between two neighboring basins of attraction is at least 9×10^5 s at room temperature and 7×10^{-4} s at 300 °C. Therefore, at temperatures lower than 300 °C, an extra-adatom would be practically trapped within a basin

of attraction. This implies that during homoepitaxial growth at $T < 300$ °C, incoming atoms would eventually be added to the same basin of attraction and bind together to form a cluster. Since neither the adatoms nor the extra-adatoms are close to bulk lattice positions, we expect that the small clusters that will be formed in each basin of attraction will resemble amorphous nuclei [4].

In order to understand epitaxial growth for $T > 300$ °C, it is necessary to investigate the microscopic kinetic pathways of island formation. While this must be based on detailed calculations for the various possibilities, the results we have obtained so far (table I) already provide an important clue on the growth process. As the number of extra-adatoms increases during the epitaxial growth process, we expect that the surface energy will increase rapidly with the extra-adatom coverage. This high-energy surface covered by extra-adatoms will subsequently change into more favorable lower-energy structures. The most likely structural changes would be the formation of clusters (such as dimer, trimer, etc.) near the adatom sites. We expect the cluster structures to be energetically favored over the isolated extra-adatoms. The clusters must then combine to form the nucleus of the next layer, a topic which is currently under investigation.

***

This work was supported by the Office of Naval Research, Contract #N00014-95-1-0350. The manuscript was prepared in part during a visit by one of us (KC) to the Center for Theoretical Physics, Seoul National University, Korea; partial financial support from this institution is gratefully acknowledged.

REFERENCES

[1] For extended references on recent theoretical and experimental work see Kaxiras E., *Comput. Mat. Sci.*, **6** (1996) 158.

[2] Kaxiras E. and Erlebacher J., *Phys. Rev. Lett.*, **72** (1994) 1714.

[3] In the case of Si(111)-(7 × 7) the term "adatoms" has been used in the literature to describe one of the most important features of the *stable* surface structure (see fig. 1). In order to distinguish the *added* atoms from the atoms that are part of the stable surface reconstruction, we will refer to the former as "extra-adatoms", reserving the term adatoms for the latter, to conform with the literature. When necessary, we refer to adatoms that are part of the stable surface reconstruction as "intrinsic" adatoms, to emphasize the difference.

[4] Köhler U., Demuth J. E. and Hamers R. J., *J. Vac. Sci. Techonol. A*, **7** (1989) 2860.

[5] Uchida H., Huang D. H., Yoshinobu J. and Aono M., *Surf. Sci.*, **287/288** (1993) 1056.

[6] Car R. and Parrinello M., *Phys. Rev. Lett.*, **55** (1985) 2471.

[7] Payne M. C., Teter M. P., Allen D. C., Arias T. A. and Joannopoulos J. D., *Rev. Mod. Phys.*, **64** (1992) 1045.

[8] Brommer K. D., Larson B. E., Needels M. and Joannopoulos J. D., *Comp. Phys.*, **7** (1993) 350.

[9] Rappe A. M., Rabe K., Kaxiras E. and Joannopoulos J. D., *Phys. Rev. B*, **41** (1990) 1227.

[10] Kleinman L. and Bylander D. M., *Phys. Rev. Lett.*, **48** (1982) 1425.

[11] Monkhorst H. J. and Pack J. D., *Phys. Rev. B*, **13** (1976) 5188.

[12] We refer to the positions of the extra-adatom as "X_n-type" ($X_n = B_2, H_3, T_4$) because they are not identical to the corresponding positions of surface adatoms, yet they share certain characteristics with them in terms of coordination, if the presence of the surface adatoms is neglected.

[13] Cho K. and Joannopoulos J. D., *Phys. Rev. Lett.*, **71** (1993) 1387.

[14] Tersoff J. and Hamman D. R., *Phys. Rev. Lett.*, **50** (1983) 1998.